SPANDIDOS PUBLICATIONS

ONCOLOGY REPORTS 29: 713-719, 2013

Mesenchymal stem cells seldomly fuse with hepatocellular carcinoma cells and are mainly distributed in the tumor stroma in mouse models

GUO-CAI LI[1,2], QING-HAI YE[1], QIONG-ZHU DONG[1], NING REN[1], HU-LIANG JIA[1] and LUN-XIU QIN[1]

[1]Liver Cancer Institute and Zhongshan Hospital, Institute of Biomedical Science, Fudan University, Shanghai; [2]GaoXin Hospital, Xi'an JiaoTong University, Xi'an, Shanxi, P.R. China

Received October 12, 2012; Accepted November 20, 2012

DOI: 10.3892/or.2012.2174

Abstract. Mesenchymal stem cells (MSCs) can have an effect on the growth and metastasis of human malignancies, including hepatocellular carcinoma (HCC); however, their mechanisms of action are not yet fully understood. The cell fusion of stem cell derived from bone marrow with other cells has been increasingly emphasized. The purpose of this study was to investigate the distribution of MSCs in mouse models of HCC, as well as the cell fusion between MSCs and HCC cells. We labeled HCC cells and MSCs with green fluorescence protein (GFP), red fluorescence protein (RFP), 4',6-diamidino-2-phenylindole (DAPI) and 5-bromo-2'-deoxyuridine (BrdU). We found that MSCs fused with HCC cells at a low frequency *in vitro*. MSCs were found to be merged into HCC tissues after intravenous injection, and compared with the mice not injected with MSCs, the MSCs were mainly distributed in the tumor stroma; Following the injection of the MSCs, the tumor stroma was found to have expanded in size, and the rate of pulmonary metastasis in the MSC-injected group was significantly lower (20%) compared to that in the group not injected with MSCs (100%, P=0.01). These data suggest that cell fusion between MSCs and HCC after engraftment is not one of the main mechanisms of action of the MSCs, while stromal differentiation is a major mechanism of action of the MSCs, leading to the inhibition of the pulmonary metastasis of HCC.

Introduction

Mesenchymal stem cells (MSCs) are marrow-derived non-hematopoietic precursor cells that contribute to the maintenance and regeneration of connective tissues through engraftment (1). *In vivo* engraftment is not only an intrinsic function of MSCs but also depends on appropriate external signals produced by the tissue microenvironment (2). Over the years, the correlation between bone marrow-derived stem cells and cancers has been increasingly emphasized. Cancer is increasingly being viewed as a stem cell disease (3), and a large body of convincing evidence has shown MSCs can home to the tumor site and play an important role in tumor progression (1,4-6). The mechanisms of action of MSCs are related to tumor angiogenesis (7) and immunosuppression (8).

Hepatocellular carcinoma (HCC) is a lethal malignancy with an extremely poor prognosis due to a high rate of tumor recurrence after surgery and intra-hepatic metastases (9,10). It has been reported that bone marrow stem cells are a source of liver oval cells (11), and that transplanted bone marrow can regenerate liver cells (12,13). In our previous study, we found that MSC injection inhibited the pulmonary metastasis of HCC (14). However, the distribution and mechanisms of action of MSCs after injection have not been well documented and the majority of studies have concentrated on benign disease.

Cell fusion is a highly regulated and dramatic cellular event that is required for development and homeostasis. It has been reported that cell fusion events involving bone marrow-derived cells (BMDCs) commonly occur after different types of tissue damage and play a crucial role in tissue restoration (15,16). A number of studies have suggested that cell fusion is the main mechanism of action after stem cell transplantation other than transdifferentiation. Moreover, the broad differentiation potential of bone marrow cells in most cases is a consequence of cell fusion (15,17).

Therefore, taking into account the above data, we hypothesized that MSCs may affect HCC progression by fusing with cancer cells. In this study, we injected labeled MSCs into mice with HCC, in order to observe the *in vivo* distribution of MSCs and the cell fusion between MSCs and HCC cells.

Materials and methods

Cell lines. The MSC cell line was obtained from ScienCell Research Laboratories (Carlsbad, CA, USA), which was isolated from human bone marrow, and characterized by immunofluorescence with CD44 and CD90 antibodies, and

Correspondence to: Professor Lun-Xiu Qin, Liver Cancer Institute and Zhongshan Hospital, Institute of Biomedical Science, Fudan University, 180 Feng Lin Road, Shanghai 200032, P.R. China
E-mail: lx_qin@yahoo.com.cn

Key words: cell fusion, hepatocellular carcinoma, mesenchymal stem cells, distribution, stroma

lipid staining after differentiation. The fifth passage MSCs did not express the surface marker, CD34; they expressed low levels of fetal liver kinase-1 (Flk-1) and higher levels of CD29 and CD105. Quantitative RT-PCR showed that the MSCs expressed octamer-binding transcription factor-4 (OCT-4) and Flk-1. They were cultured in Alpha Minimum Essential Medium (α-MEM, Gibco) supplemented with 10% fetal bovine serum (FBS, Gibco) and 100 U/ml penicillin/streptomycin solution. The fifth to eighth passage cells were used in the following experiments.

MHCC97-H is human HCC cell line with a higher metastatic potential (18,19). These cells were cultured in high glucose Dulbecco's modified Eagle's medium (H-DMEM, Gibco), supplemented with 10% FBS at 37˚C in a humidified incubator containing 5% CO_2.

Labeling of MSCs and liver cancer cells. MHCC97-H cells were labeled with green fluorescence protein (GFP) by transfection with the plasma vector, pEGFP-N1 (Clontech). Lipofectamine 2000 which mediated the highest transfection rates was used as a transfection agent. After 2 weeks of selection with G418 (800 μg/ml), the individual G418-resistant clones were picked up and subcultured. Finally, a stable eukaryotic cell line with the highest fraction of EGFP expression was obtained (GFP-MHCC97-H).

MSCs were labeled with red fluorescence protein (RFP) and GFP by transfection with the plasma vector, pERFP-N1 (Clontech), and after 2 weeks of selection with G418 (400 μg/ml), stable RFP-MSCs and GFP-MSCs were then acquired, respectively.

MSCs were labeled with 4',6-diamidino-2-phenylindole (DAPI, Vector Laboratories) according to the manufacturer's instructions.

MSCs were also labeled with 5-bromodeoxyuridine (BrdU, Sigma) according to the manufacturer's intuductions. For BrdU labeling, MSCs were cultured for 15 min in the presence of 2 mM BrdU, washed and expanded for 2 additional passages before being injected into the mice. This procedure labeled 70-80% of the MSCs.

Co-culture of MSCs and liver cancer cells. To evaluate the *in vitro* cell fusion between MSCs and HCC cells, the GFP-MHCC97-H cells were co-cultured with DAPI-MSCs at a ratio of 5:1 in a 6-well plate. After 4 days, the culture was observed under a fluorescence microscope. Similarly, GFP-MHCC97-H cells and RFP-MSCs were also co-cultured at a ratio of 5:1 and observed under a microscope.

An Axioplan Epifluorescence microscope (Carl Zeiss, Oberkochen, Germany) was used and images were obtained using a DC300 digital video camera (Leica). Optical images were acquired using a DMR microscope connected to a DC300 video camera (Leica).

Co-culture of GFP-MSCs and RFP-MSCs. RFP-MSCs and GFP-MSCs were co-cultured at a ratio of 1:1 in a 6-well plate. The culture was observed under a fluorescence microscope to evaluate the *in vitro* cell fusion of the MSCs.

Cytoimmunochemistry. MSCs ($2x10^5$) were plated and cultured in 6-well plate. When the cells had reached 60% confluency, they were fixed with 100% methanol, permeabilized with 0.5% Triton X-100, and sequentially incubated with primary anti-matrix metalloproteinase (MMP)2 or primary anti-MMP9 monoclonal antibodies and anti-mouse immunoglobulin (Ig) coupled with horseradish peroxidase (HRP). The cells were then stained with 3,3'-diaminobenzidine (DAB) and counterstained with hematoxylin.

Transwell assay for in vitro migration of MSCs. In vitro invasion assay was performed as follows: briefly, 80 μl of serum-free α-MEM-diluted Matrigel (0.8 mg/ml) was added to the Transwell filters (8.0μm pore size) of a Boyden chamber (Costar, MA, USA) and incubated at 37˚C for 2 h to form matrix gel. MSCs ($1x10^6$) were cultured in FBS-free α-MEM for 24 h, and subsequently the cells were collected and counted. Cells ($2x10^5$) were re-suspended with α-MEM and seeded in the upper well of Transwell chamber, a mixture of 600 μl of α-MEM with 10% fetal calf serum (FCS) was added to the lower chamber, serving as the chemoattractant. After incubation at 37˚C for 48 h, the cells that had invaded across the Matrigel and passed through the Transwell filter were stained and observed under a light microscope.

Gelatin zymography detection of MMP2 and MMP9 activities. Equal amounts of protein from the MSCs, MHCC97-H and MHCC97-L cells (HCC cells with lower metastasis) were mixed with SDS buffer and incubated for 20 min at 37˚C. After incubation, samples (30 μg/lane) were added onto a 4.5% (w/v) stacking polyacrylamide gel and separated on a 7.5% (w/v) polyacrylamide gel containing 1 mg/ml gelatin for the detection of MMP2 and MMP9 activities. After electrophoresis, the gels were soaked in 2.5% Triton X-100 for 1 h to remove SDS and incubated for 16 h at 37˚C in 50 mM Tris-HCl (pH 7.6) containing 150 mM NaCl, 10 mM $CaCl_2$ and 0.02% NaN_3. Finally, the gels were stained for 1 h in 45% methanol/10% acetic acid containing 0.5% Coomassie brilliant blue G250. Proteolytic activity was detected as clear bands on a blue background of the Coomassie blue staining gel.

In vivo visualization of MSCs. To detect the distribution of MSCs *in vivo*, we subcutaneously injected $6x10^6$ GFP-MHCC97-H cells into nude mice (n=4). When the nodular tumors were formulated, we injected $5x10^5$ of human DAPI-MSCs into the tail veins of the mice. Four days after the injection, the mice were sacrificed, the subcutaneous tumor tissues, livers and lungs were removed and embedded with 1:4 dilution of optimum cutting temperature (OCT) compound in phosphate-buffered saline (PBS). Fresh-frozen tumor sections (5-μm thick) were mounted on glass slides, and the distribution of DAPI-MSCs was observed under a fluorescence microscope. These experiments were approved by the Shanghai Medical Experimental Animal Care Commission.

We also orthotopically implanted tissues of subcutaneous tumor into the livers of 10 nude mice, and 15 days after the implantation, 5 out of the 10 mice were intravenously injected with $5x10^5$ of human BrdU-MSCs 3 times per week. The other 5 mice were injected with PBS as the controls. After 20 days, the tumors, livers and lungs were removed and fixed in paraformaldehyde and embedded in paraffin wax. Paraffin sections (5-μm-thick) were mounted on glass slides.

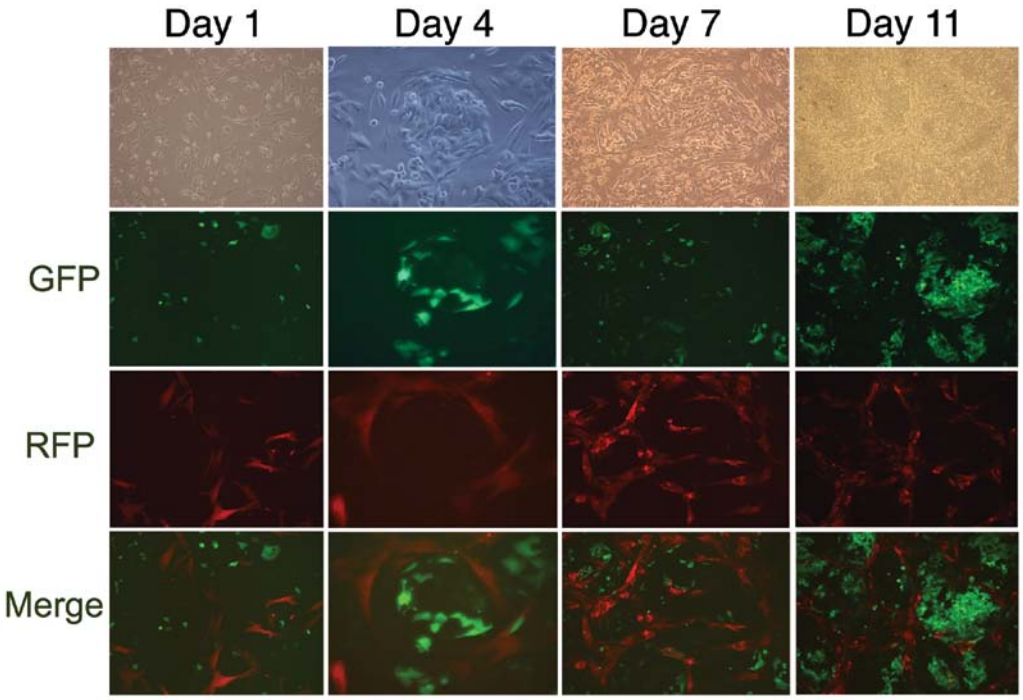

Figure 1. Co-culture of RFP-MSCs and GFP-MHCC97-H. RFP-MSCs (red) and GFP-MHCC97-H cells (green) were co-cultured at a ratio of 5:1, and the culture were observed under a fluorescence microscope from day 4 to 11. The cultures were well grown. The cell fusion was not evident, while, MSCs interweaved and partitioned cancer cells; the formation was similar to the *in vivo* tumor structures. The top panel denotes the cultures observed under a phase-contrast microscope (magnification, x20).

The tumor and liver slides were deparaffinized and rehydrated over 10 min through a graded alcohol series to deionized water. Subsequently, 1% Antigen Unmasking Solution (Vector Laboratories) was added and the slides were microwaved to enhance antigen retrieval, followed by immunostaining with primary mouse anti-human antibody against BrdU (Sigma). Goat anti-mouse IgG-peroxidase (A9917, Sigma) or Cy3-Goat anti-mouse IgG were used as the secondary antibodies.

Analysis of pulmonary metastasis. Lung samples were sliced into 20 sections of 5 μm thickness, and a 50-μm interval between 2 successive sections. After staining with hematoxylin and eosin (H&E), the sections were independently observed under a microscope by 2 pathologists to evaluate pulmonary metastasis.

Statistical analysis. The data were analyzed using SPSS 11.5 software (SPSS Corp., Chicago, IL). The Student's t-test was used to analyze the differences in tumor weight. Fisher's exact test was used for the comparison of the ratio involved. All statistical tests were two-sided and $P<0.05$ was considered to indicate a statistically significant difference.

Results

MSCs fuse with HCC cells in vitro at a low frequency. After the co-culture of GFP-MHCC97-H with RFP-MSCs, and the co-culture of GFP-MHCC97-H with DAPI-MSCs, the culture formation mimicked the *in vivo* tumor structures. MSCs gradually circled and partitioned cancer cells (Fig. 1). Cell fusion was observed in the cultures on the 4th day, and binucleated or yellow fluorescent hybrid cells had formed. However, the cells fused at a very low frequency (approximately 4-5 GFP^+ RFP^+ cells and 4-5 binucleated cells were observed per microscopic sight; x20), and the cell fusion did not obviously increase in the following days (Fig. 2A and B).

MSCs spontaneously fuse with each other in vitro. When GFP-MSCs and RFP-MSCs were co-cultured for 4 days, cell fusion was also observed in the culture; however, the cell fusion was also generated at a low frequency and did not increase in the following time-periods (Fig. 2C).

Detection of MMP expression and invasive capability of MSCs. We found that MSCs expressed MMP2 at a low level (Fig. 3A), but highly expressed MMP9 (Fig. 3B), as shown by immunocytochemistry staining with MMP2 and MMP9 monoclonal antibodies. MSCs infiltrated through the Matrigel, as shown by *in vitro* Transwell assay (Fig. 3C). The zymographic pattern showed that the MSCs had a higher activity of MMP9 than the MHCC97-L cells (HCC cells with a lower metastatic potential) (Fig. 3D) (17,22).

DAPI-MSCs home to tumor site. Four days after injecting DAPI-MSCs into the mice, we found that fewer MSCs had engrafted the heart, spleen, kidneys and bone marrow, (Fig. 4A) while, more DAPI-MSCs were present in the tumor site compared with the normal liver tissues (Fig. 4B). More DAPI-MSCs were present in the site of pulmonary metastasis compared with the normal lung tissues (Fig. 4C).

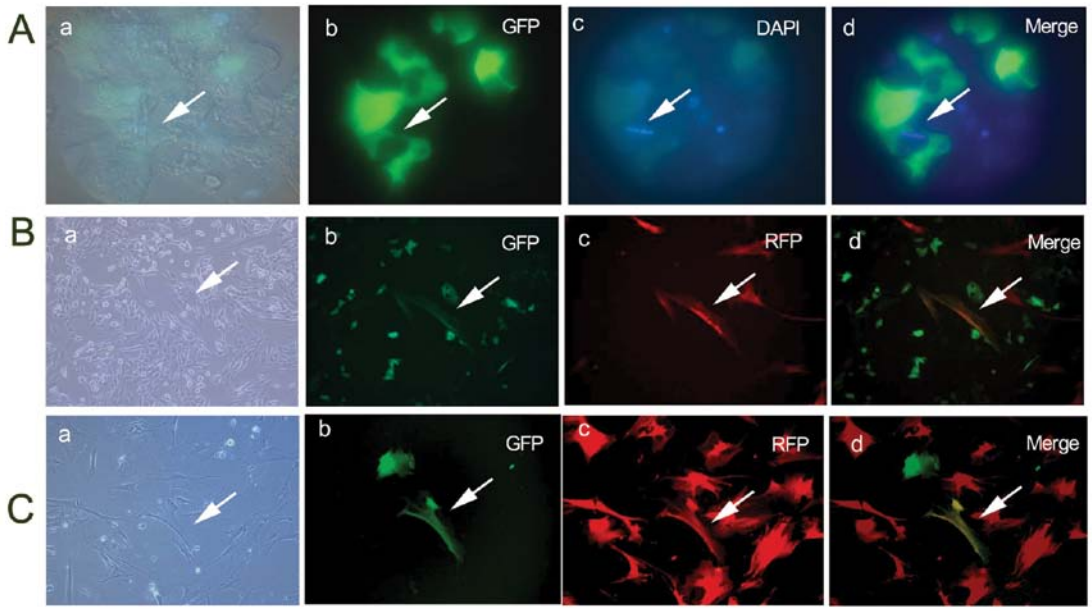

Figure 2. Cell fusion between MSCs and MHCC97-H cells, as well as cell fusion among MSCs observed under a phase contrast and fluorescence microscope. (A) After 4 days co-culture, RFP-MSCs (red) fused with GFP-MHCC97-H cells (green), and the RFP^+ GFP^+ fusion cells (yellow) were observed (magnification, x20). (B) After 4 days co-culture, DAPI-MSCs (blue) fused with GFP-MHCC97-H cells (green), and binucleated cells were observed in the culture. Arrows denote the fused cells (magnification, x40). (C) RFP-MSCs and GFP-MSCs were co-cultured at a ratio of 1:1 in a 6-well plate, the cell fusion was spontaneously generated among the MSCs (magnification, x20).

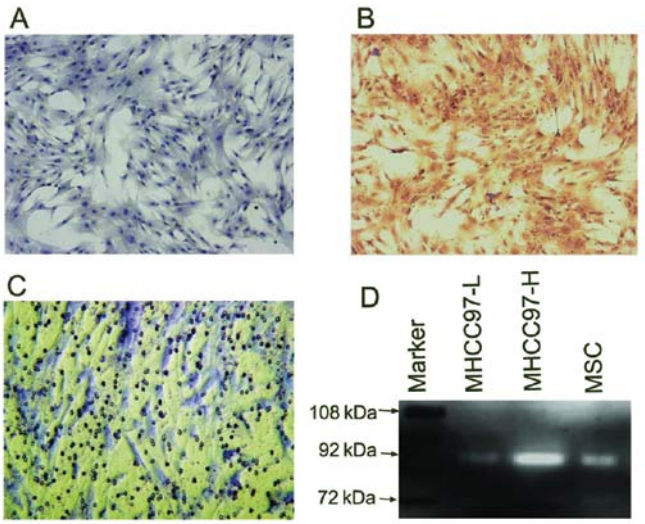

Figure 3. Detection of invasive capability of MSCs. (A and B) MSCs expressed (A) MMP2 at lower levels, but highly expressed (B) MMP9, as shown by immunohistochemistical staining with MMP2 and MMP9 monoclonal antibodies. (C) MSCs infiltrated through the Matrigel, as shown by *in vitro* Transwell assay. The cells were stained with Giemsa. (D) Zymographic pattern of MSCs. MSCs had a higher activity of MMP-9 (92 kDa, latent form of MMP9; 72 kDa, latent form of MMP2). The MHCC97-H and MHCC97-L cells were used as the controls.

Table I. Effect of MSCs on tumor growth and invasion of HCC.

	MSC injection	No. of animals	(Mean ± SE)	P-value
Tumor weight	Yes	5	2.63±0.29	0.163
	No	5	3.10±0.21	
Rate (%)	Yes	5	20%	0.010
	No	5	100%	
No. of lesions	Yes	5	0.60±0.60	0.008
	No	5	3.00±0.71	
No. of cells	Yes	5	7.60±7.60	0.029
	No	5	58.00±17.36	

The Student's t-test was used to assess the statistical difference of tumor weight, no. of lesions and no. of cells between the group injected with MSCs and the group not injected with MSCs. The rate of pulmonary metastasis in each group was analyzed by Fisher's exact test. Rate, rate of pulmonary metastasis; no. of lesions, total number of metastatic lesions in lungs; no. of cells, total number of metastatic cells in the lungs; SE, standard error.

MSCs distributed in tumor stroma. Twenty days after the BrdU-MSC injection, we did not find any more binucleated cells in the tumor tissuses and the cells were mainly distributed in the tumor stroma. Moreover, we found that the components of the tumor stroma had increased compared to the tumors not injected with MSCs, as shown by immunostaining with Brdu (Fig. 5A-D).

Injection of MSCs affects the invasion of HCC cells. After the *in vivo* injection of MSCs, we also found that the invasive capability of the HCC cells significantly decreased. The rate of pulmonary metastasis was 20% in the group injected with MSCs and 100% in the group not injected with MSCs (P=0.01). The total number of metastatic cells, as well as the total number of metastatic lesions in the lungs had decreased (Table I).

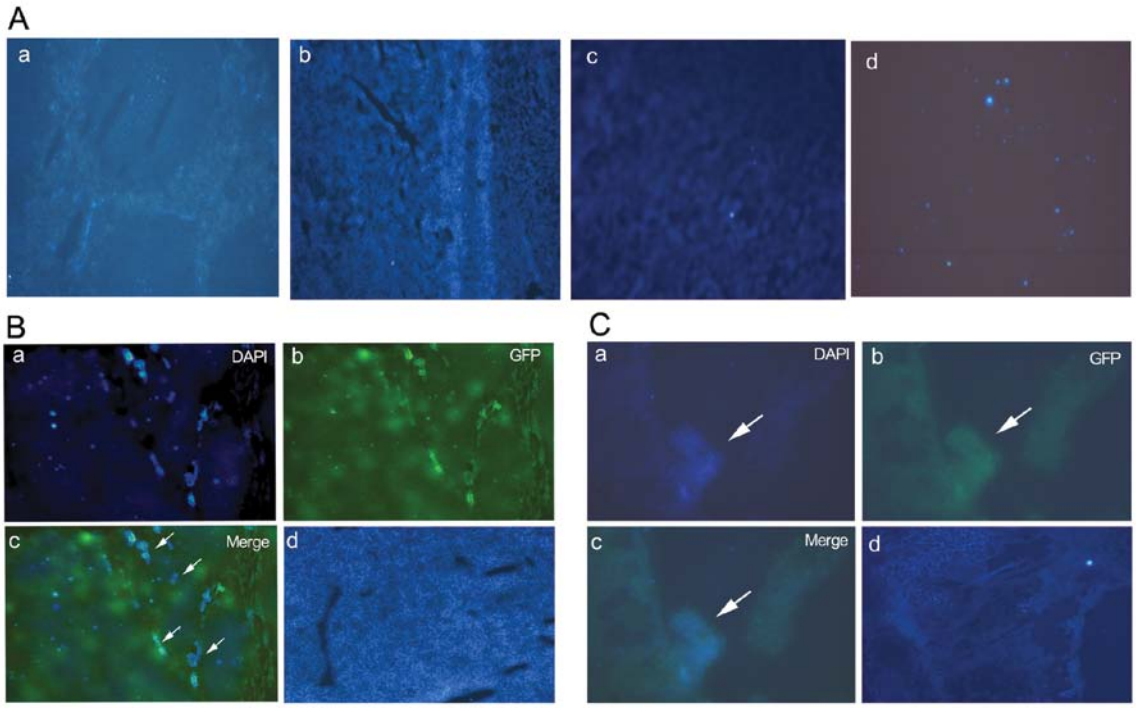

Figure 4. Distribution of MSCs in mice bearing tumors. (A) Distribution of DAPI-MSCs (blue) in mouse (a) spleen, (b) heart, (c) kidneys and (d) bone marrow (magnification, x10). (B) More DAPI-MSCs (blue) homed to tumor tissues formed by GFP-MHCC97-H cells (green) than to normal liver tissues (d) (magnification, x20). Cell fusion was also observed found (arrow denote). (C) More DAPI-MSCs (blue) home to pulmonary metastatic sites formed by GFP-MHCC97-H cells (green) than to normal lung tissues (d). Arrows denote metastases formed in lungs (magnification, x10).

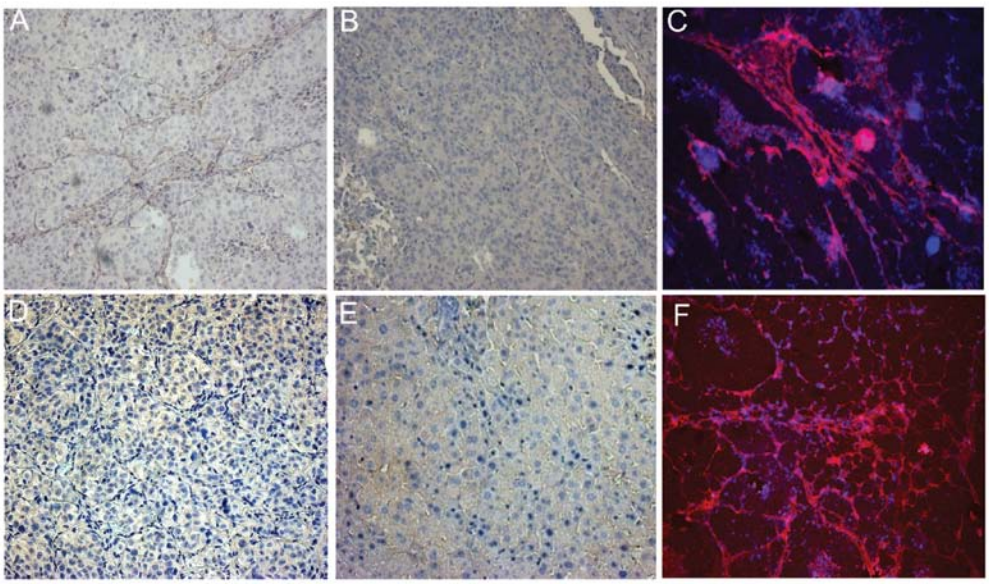

Figure 5. MSC were mainly distributed in the tumor stroma. (A and B) Immunostaining with anti-BrdU antibody, BrdU-MSCs were mainly found in the tumor stroma. (A) Sample without BrdU-MSC injection was immunostained with anti-BrdU antibody as the negative control. (B) DAB staining. (C) Similarly, using Cy3 labeling anti-BrdU antibody, BrdU-MSCs were mainly observed in the tumor stroma (magnification, x10). (D and E) As shown by immunostaining with anti-BrdU antibody, (D) MSC-injected samples had an enlarged tumor stroma compared to (E) the samples not injected with MSCs (magnification, x10). (F) Using Cy3 labeled anti-BrdU antibody, BrdU-MSCs increased the tumor stroma size. Red, Cy3; blue, nuclei counter staining with DAPI.

Discussion

Although cell fusion has been emphasized in other studies, few hybrid cells were observed in our experiment both *in vitro* and *in vivo*, and cell fusion mainly occurred 4-5 days after *in vitro* co-culture; even between the MSCs themselves, cell fusion spontaneously occurred at a low level (Fig. 2C). Our results suggested that cell fusion was not a major mechanism by which MSCs

influence HCC. These results were consistent with the report that engrafted MSCs do not fuse with somatic cells in rats, as shown by fluorescence *in situ* hybridization (20). In another study (21), binucleated heterokaryons were not observed in the regenerated liver after MSC transplantation. The efficiency of *in vivo* somatic fusion is possibly influenced by a number of factors. BMDCs have been found to regenerate liver tissue by fusing with existing hepatocytes at a low frequency (12,22,23). Moreover, it is haematopoietic stem cells (HSCs), rather than MSCs, that are more often associated with the phenomena of cell fusion (11,22-25).

MMPs are important enzymes that mediate endothelial cell invasion and the homing of stem cells (25,26). It has been reported that MMP9 is one of the elements required to break down basement membranes and to provide a road map for the homing of HSCs (25). In this study, MSCs expressed a high level of MMP9, suggesting that the homing of MSCs also correlates with MMP9. We also observed a higher invasive capability of MSCs *in vitro* by Transwell assay and a higher number of MSCs distributed in the tumor site rather than the normal liver tissues. These data suggest that tumor microenvironment may provide a special niche for the homing of engrafted MSCs.

Our results demonstrated that MSCs were mainly distributed in the tumor stroma and differentiated into stromal cells; which is in disagreement with the hepatocellular differentiation of MSCs, and which reflects a limited differentiation of MSCs in the microenvironment of HCC. The views regarding the differentiation capability of MSCs are controversial. The self-renewal and proliferative capacity of adult stem cells is very limited (27) and only a limited proportion of adult stem cells isolated from post-natal tissues are capable of differentiating into the hepatic lineage (28,29). The hepatic differentiation of MSCs *in vitro* may be due to the ideal milieu created by humans MSCs which are chemically defined, either by the use of serum-free or synthetic serum replacements (30), with the possible supplementation of specific recombinant cytokines, growth factors and extracellular matrix (ECM) substratum.

The tumor stroma is composed of myofibroblasts and fibroblasts which produce the extracellular matrix supporting the tumor structure and influences invasiveness (31-33). The tumor stroma has been regarded as a more dynamic component of tumors. In our study, we found that MSCs were mainly distributed in the tumor stroma. Therefore, the engrafted MSCs may be capable of changing the tumor microenvironment, influencing tumor progression in a complex manner associated with the secretion of growth factors, chemokines and cytokines (6,34,35).

In conclusion, our results suggest that after transplanting MSCs in HCC tumors, cell fusion is not the major mechanism of action of the MSCs; MSCs mainly engraft into the tumor tissues and differentiate into tumor stromal cells and thus regulate the formation of the stroma. The data presented in this study may provide novel potential methods for the application of anticancer therapies.

Acknowledgements

The present study was supported in part by the China National Key Projects for Infectious Disease (2008ZX10002-021), the China National Natural Science Foundation for Distinguished Young Scholars (30325041) and the China National High-tech Research and Development Program (863 Program) (2006AA02Z473), and the Program of Shanghai Subject Chief Scientist (08XD1400800). We would like to thank Dr Qiong Xue, Dr Dongmei Gao and Dr Jun Chen for assistance with the animal experiments, Dr Ruixia Sun and Dr Jie Chen for helpful suggestions for the cell culture experiments and Dr Haiying Zeng and Dr Tengfang Zhu for assistance with the pathological experiments.

References

1. Studeny M, Marini FC, Dembinski JL, Zompetta C, Cabreira-Hansen M and Bekele BN: Mesenchymal stem cells: potential precursors for tumor stroma and targeted-delivery vehicles for anticancer agents. J Natl Cancer Inst 96: 1593-1603, 2004.
2. Horwitz EM, Prockop DJ, Fitzpatrick LA, Koo WW, Gordon PL and Neel M: Transplantability and therapeutic effects of bone marrow-derived mesenchymal cells in children with osteogenesis imperfecta. Nat Med 5: 309-313, 1999.
3. Beachy PA, Karhadkar SS and Berman DM: Tissue repair and stem cell renewal in carcinogenesis. Nature 432: 324-331, 2004.
4. Fierro FA, Sierralta WD, Epuñan MJ and Minguell JJ: Marrow-derived mesenchymal stem cells: role in epithelial tumor cell determination. Clin Exp Metastas 21: 313-319, 2004.
5. Zhu W, Xu W, Jiang R, Qian H, Chen M, Hu J, Cao W, Han C and Chen Y: Mesenchymal stem cells derived from bone marrow favor tumor cell growth in vivo. Exp Mol Pathol 80: 267-274, 2006.
6. Karnoub AE, Dash AB, Vo AP, Sullivan A, Brooks MW, Bell GW, Richardson AL, Polyak K, Tubo R and Weinberg RA: Mesenchymal stem cells within tumour stroma promote breast cancer metastasis. Nature 449: 557-563, 2007.
7. Reyes M, Dudek A, Jahagirdan B, Koodie L, Marker PH and Verfaillie CM: Origin of endothelial progenitors in human postnatal bone marrow. J Clin Invest 109: 337-346, 2002.
8. Djouad F, Plence P, Bony C, Tropel P, Apparailly F, Sany J, Noël D and Jorgensen C: Immunosuppressive effect of mesenchymal stem cells favors tumor growth in allogeneic animals. Blood 102: 3837-3844, 2003.
9. Portolani N, Coniglio A, Ghidoni S, GiovanellMi A, Benetti G and Tiberio A: Early and late recurrence after liver resection for hepatocellular carcinoma: prognostic and therapeutic implications. Ann Surg 243: 229-235, 2006.
10. Ye QH, Qin LX, Forgues M, He P, Kim JW and Peng AC: Predicting hepatitis B virus-positive metastatic hepatocellular carcinomas using gene expression profiling and supervised machine learning. Nat Med 9: 416-423, 2003.
11. Alison MR and Lovell MJ: Liver cancer: the role of stem cells. Cell Prolif 38: 407-421, 2005.
12. Vassilopoulos G, Wang PR and Russell DW: Transplanted bone marrow regenerates liver by cell fusion. Nature 422: 901-904, 2003.
13. Wang X, Willenbring H, Akkari Y, Torimaru Y, Foster M, Al-Dhalimy M, Lagasse E, Finegold M, Olson S and Grompe M: Cell fusion is the principal source of bone-marrow-derived hepatocytes. Nature 422: 897-901, 2003.
14. Li GC, Ye QH, Xue YH, Sun HJ, Zhou HJ, Ren N, Jia HL, Shi J, Wu JC, Dai C, Dong QZ and Qin LX: Human mesenchymal stem cells inhibit metastasis of a hepatocellular carcinoma model using the MHCC97-H cell line. Cancer Sci 101: 2546-2553, 2010.
15. Nygren JM, Jovinge S, Breitbach M, Säwén P, Röll W, Hescheler J, Taneera J, Fleischmann BK and Jacobsen SE: Bone marrow-derived hematopoietic cells generate cardiomyocytes at a low frequency through cell fusion, but not transdifferentiation. Nat Med 10: 494-501, 2004.
16. Chen EH, Grote E, Mohler W and Vignery A: Cell-cell fusion. FEBS Lett 581: 2181-2193, 2007.
17. Ying QL, Nichols J, Chambers I and Smith A: BMP induction of Id proteins suppresses differentiation and sustains embryonic stem cell self-renewal in collaboration with STAT3. Cell 115: 281-292, 2003.
18. Li Y, Tang Y, Ye L, Liu B, Liu K and Chen J: Establishment of a hepatocellular carcinoma cell line with unique metastatic characteristics through in vivo selection and screening for metastasis-related genes through cDNA microarray. J Cancer Res Clin Oncol 129: 43-51, 2003.

19. Li Y, Tang ZY, Ye SL, Liu YK, Chen J and Xue Q: Establishment of cell clones with different metastatic potential from the metastatic hepatocellular carcinoma cell line MHCC97. World J Gastroenterol 7: 630-636, 2001.
20. Sato Y, Araki H, Kato J, Nakamura K, Kawano Y, Kobune M, Sato T, Miyanishi K, Matsuura A, Hamada H and Niitsu Y: Human mesenchymal stem cells xenografted directly to rat liver are differentiated into human hepatocytes without fusion. Blood 106: 756-763, 2005.
21. Kozorovitskiy Y and Gould E: Stem cell fusion in the brain. Nat Cell Biol 5: 952-954, 2003.
22. Wang X, Willenbring H and Akkari Y: Cell fusion is the principal source of bone-marrow-derived hepatocytes. Nature 42: 2897-2901, 2003.
23. Alvarez-Dolado M, Pardal R, Garcia-Verdugo JM, Fike JR, Lee HO, Pfeffer K, Lois C, Morrison SJ and Alvarez-Buylla A: Fusion of bone-marrow-derived cells with Purkinje neurons, cardiomyocytes and hepatocytes. Nature 425: 968-973, 2003.
24. Menthena A, Deb N, Oertel M, Grozdanov PN, Sandhu J, Shah S, Guha C, Shafritz DA and Dabeva MD: Bone marrow progenitors are not the source of expanding oval cells in injured liver. Stem Cells 22: 1049-1061, 2004.
25. Kaplan RN, Riba RD, Zacharoulis S, Bramley AH, Vincent L, Costa C, Daniel DM, Ruggero D and Shmelkov SV: VEGFR1-positive haematopoietic bone marrow progenitors initiate the pre-metastatic niche. Nature 438: 820-827, 2005.
26. Ball SG, Shuttleworth AC and Kielty CM: Circulating fibrocytes: collagen-secreting cells of the peripheral blood. Int J Biochem Cell Biol 36: 598-606, 2004.
27. Iakova P, Awad SS and Timchenko NA: Aging reduces proliferative capacities of liver by switching pathways of C/EBPalpha growth arrest. Cell 113: 495-506, 2003.
28. Wagemaker G, Neelis KJ and Wognum AW: Surface markers and growth factor receptors of immature hemopoie tic stem cell subsets. Stem Cells 13 (Suppl 1): 165-171, 1995.
29. Zheng YW and Taniguchi H: Diversity of hepatic stem cells in the fetal and adult liver. Semin Liver Dis 23: 337-348, 2003.
30. Goldsborough MD, Tilkins ML, Price PJ, Lobo-Alfonso J, Morrison JR and Stevens ME: Serum-free culture of murine embryonic stem (ES) cells. Focus 20: 8-12, 1998.
31. Desmouliere A, Guyot C and Gabbiani G: The stroma reaction myofibroblast: a key player in the control of tumor cell behavior. Int J Dev Biol 48: 509-517, 2004.
32. De Wever O and Mareel M: Role of tissue stroma in cancer cell invasion. J Pathol 200: 429-447, 2003.
33. Direkze NC and Alison MR: Bone marrow and tumour stroma: an intimate relationship. Hematol Oncol 24: 189-195, 2006.
34. Littlepage LE, Egeblad M and Werb Z: Coevolution of cancer and stromal cellular responses. Cancer Cell 7: 499-500, 2005.
35. Welm AL: TGFbeta primes breast tumor cells for metastasis. Cell 33: 27-28, 2008.